

First-principles study of the incorporation and diffusion of helium in cubic zirconia

Peng Zhang^{1,2}, Yong Lu^{2,3}, Chao-Hui He¹, and Ping Zhang^{2,4*}

¹*Department of Nuclear Science and Technology,*

Xi'an Jiaotong University, Xi'an 710049, People's Republic of China

²*LCP, Institute of Applied Physics and Computational Mathematics, Beijing 100088, People's Republic of China*

³*Department of Physics, Beijing Normal University, Beijing 100875, People's Republic of China*

⁴*Center for Applied Physics and Technology, Peking University, Beijing 100871, People's Republic of China*

The incorporation and diffusion of helium (He) with and without intrinsic vacancy defects in cubic ZrO₂ are investigated through first-principles total-energy calculations, in which the projector-augmented-wave (PAW) method with the generalized gradient approximation (GGA) is used. The calculated formation energies of intrinsic point defects indicate that cubic ZrO₂ has a tolerant resistance to radiation damage. The incorporation energy of He impurity shows that it is preferable to occupy the Zr vacancy at first, whereas the solution energy suggests that He would be accommodated in the interstitial site at thermodynamic equilibrium concentration. By calculating the He migration energies corresponding to both interstitial and vacancy assisted mechanisms, we suggest that it is most likely for He to diffuse by hopping through a single vacancy. Remarkably, our calculated vacancy-assisted diffusion energy of He is consistent well with the experimental measurement.

PACS numbers: 61.72.Ji, 66.30.Jt

I. INTRODUCTION

Zirconia (ZrO₂) is a highly attractive material of great interests both scientifically and in terms of its technological applications due to its excellent mechanical, thermal, chemical, and dielectric properties [1]. For example, ZrO₂ is employed as superplastic structural ceramic that demonstrates superb strength and fracture toughness [2], and is also used as one of the best refractive engineering materials for thermal barrier coating on aeronautical and land-based gas turbine blades [3]. Additionally, the cation-doped ZrO₂ can also be used in solid oxide fuel cells and oxygen sensors [4]. Furthermore, as one of the most radiation resistant ceramic materials, ZrO₂ is applied as a promising candidate host phase for the inert matrix nuclear fuel (IMF) in order to immobilize [5] and burn up [6] the plutonium from dismantled nuclear weapons and other high level nuclear waste (HLW) caused by the actinides (e.g. ²⁴¹Am). Consequently, great attentions are needed to focus on the basic scientific research of ZrO₂.

ZrO₂ exists at least five crystalline structures with different symmetries. The monoclinic $P2_1/c$ polymorph is the only one found at ambient condition whereas the tetragonal $P4_2/nmc$ and the cubic $Fm\bar{3}m$ phases are stable above 1400 and 2600 K and the other two orthorhombic $Pbca$ and $Pnma$ phases are stable above 3 and 20 GPa, respectively [8–12]. As these five ZrO₂ structures are centrosymmetric, they are all nonpolar and nonpiezoelectric. Presently, ZrO₂ stabilized in the cubic phase with e.g. Y₂O₃ is considered as a suitable refractory host for actinide confinement used for transmutation or

high-temperature reactor projects. Large amounts of experimental measurements have been carried out to determine the stability of this material in high radiation environment. One early investigation on phase stability of ZrO₂ under fission fragment damage was reported by Wittels and Sherrill [13]. Then the evolution of radiation induced damages in ZrO₂ [14] was systematically investigated using Rutherford backscattering spectrometry and ion channeling (RBS/C), along with X-ray diffraction and transmission electron microscopy (TEM) under Xe and I ion irradiation. No amorphization of the pure ZrO₂ was observed. But Meldrum *et al.* [15] found that nanocrystalline ZrO₂ could be amorphized under Ne and Xe ion irradiation. Damage evolution, surface morphology and characteristic structural changes in He-implanted cubic ZrO₂ were extensively investigated in experiments [16–19]. Fluence dependence and thermal stability of defects in He-implanted cubic ZrO₂ was determined by slow positron implantation spectroscopy [20]. Moreover, the He damage and He effusion in fully stabilized ZrO₂ [21] was measured with neutron depth profiling (NDP) for different annealing temperatures and analyzed by electron microscopy during the various annealing stages concluding that the diffusion of He is probably caused by vacancy assisted interstitial diffusion. Besides, He migration in monoclinic and cubic yttria-stabilized ZrO₂ was also studied from non-destructive ³He depth profiling using the resonant ³He(d,p)⁴He nuclear reaction [22].

From theoretical point of view, *ab initio* methods have been employed to study the structural, electronic, mechanical, thermodynamical, and vibrational properties of ZrO₂ [1, 23–33]. Very recently, the energetics of intrinsic point defects and the influence of Al doping in ZrO₂ [34–36] have been studied to identify the dominant defects under different oxygen chemical potentials and Fermi levels. However, up to date there are no detailed investigation

*Author to whom correspondence should be addressed. E-mail: zhang_ping@iapcm.ac.cn

performed on the He incorporation and diffusion behavior in ZrO_2 through a state-of-the-art first-principles approach. To make a deep understanding of the effect of He in ZrO_2 in atomic scale is helpful for us to be more confident to validate the application of ZrO_2 in severe environment. Therefore, this is the main purpose of the present work. In the present study, first the behavior of He in cubic ZrO_2 is investigated by determining the formation energy of point defects. Then the incorporation energy of He into different sites of the lattice is calculated, through which the most favorable incorporation site is determined. By taking thermodynamic equilibrium into account, the solubility of He is also evaluated. After exploration of the stability of He, we subsequently concentrate on the diffusion mechanism of He in ZrO_2 by calculating energy barriers and migration pathways between two trapping sites. After comparison of calculated results for different postulated mechanisms, we present the viable diffusion mechanism of He in ZrO_2 matrix.

II. COMPUTATIONAL METHOD

The density functional theory (DFT) total energy calculations are self-consistently performed in the framework of the frozen core all-electron PAW method [37] as implemented in the Vienna ab initio simulation package (VASP) [38]. The electron exchange and correlation potentials are evaluated within the GGA introduced by Perdew, Burke, and Ernzerhof (PBE) [39]. Twelve electrons ($4s^2 4p^6 4d^2 5s^2$) for zirconium (Zr) and six electrons ($2s^2 2p^4$) for oxygen (O) are taken into account as valence electrons. To get accurate results, the cutoff energy of the plane wave expansion is set up to a high value of 800 eV, which was tested to be well converged with respect to the total energy. The integration over the Brillouin Zone (BZ) is performed with a grid of special k point-mesh determined according to the Monkhorst-Pack scheme [40]. After convergence test, $8 \times 8 \times 8$ k point-mesh is chosen to calculate the bulk properties with the total energy difference less than 1 meV per unit cell. In the present work, large supercells containing up to 96 atoms have been employed to reduce any artificial error due to the use of a smaller supercell as it will be shown later. Correspondingly, a $2 \times 2 \times 2$ k -point grid is used to sample the BZ of the 96-atom supercell for the modeling of the point defects and He impurity in ZrO_2 . Relaxation procedures at ground state are carried out according to the Gaussian broadening with a smearing width of 0.1 eV. For all defect structures, the atomic relaxation is considered to be completed when the Hellmann-Feynman forces on all atoms are less than 0.01 eV/Å. And the volume relaxation of the supercell is also calculated.

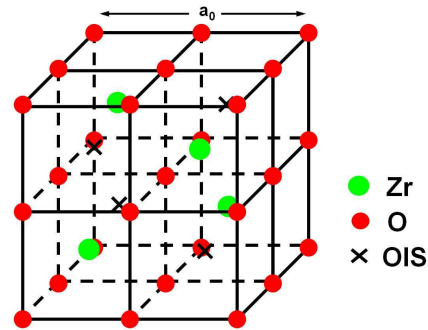


FIG. 1: Conventional unit cell of ZrO_2 . O atoms are located at the corners of small cubes, and Zr atoms are located at the center of an alternative cubes. \times indicates the octahedral interstitial site (OIS) in the lattice.

III. RESULTS AND DISCUSSIONS

A. Crystallography and bulk properties

Here, we considered the cubic phase of ZrO_2 , which is crystallized in the fluorite structure with space group $Fm\bar{3}m$ (No. 225). The Zr atoms are in the center of a cube of O atoms, while the O atoms occupy the tetrahedral sites coordinated by Zr atoms, constituting a simple cubic sublattice as shown in Fig. 1. The present optimized equilibrium lattice parameter (a) obtained by fitting the energy-volume data in the third-order Birch-Murnaghan equation of states (EOS) [41] is 5.152 Å and some other basic bulk properties calculated with this PAW method is also listed in Table 1, in fair agreement with the experimental and previous theoretical results.

B. Intrinsic point defects formation

The previous study of ZrO_2 bulk properties gives insights into the reliability of the DFT-GGA approach to model the cubic ZrO_2 . Now we turn to the study of the stability of different types of point defects in the fluorite lattice. The first-principles method allows us to consider ZrO_2 supercells containing up to hundred atoms and thus to carefully check the convergence of the defect formation energies as a function of the supercell size. Indeed, in too small a supercell and due to the periodic boundary conditions, a point defect interacts with its image in the adjacent supercell, which yields a spurious contribution to the calculated formation energy. To check this convergence, we have considered supercells representing repetition of the elementary cubic cell according to the following repetition pattern: $1 \times 1 \times 1$ (12 atoms), $2 \times 1 \times 1$ (24 atoms), $2 \times 2 \times 1$ (48 atoms), $2 \times 2 \times 2$ (96 atoms), $3 \times 2 \times 2$ (144 atoms), $3 \times 3 \times 2$ (216 atoms), $3 \times 3 \times 3$ (324 atoms). The defects are explicitly investigated in the calculation of formation energy as follows: vacancies, interstitials at OIS, Frenkel pair and Schottky defect.

TABLE I: Calculated equilibrium lattice parameter a_0 (Å), bulk modulus B_0 (GPa), and cohesive energy E_{coh} (eV) of fluorite ZrO_2 at ground state. For comparison, available experimental values and other theoretical results are also listed.

Parameter	Present work	Previous calculation	Experiment
a_0 (Å)	5.152	5.130 ^a , 5.128 ^b , 5.116 ^c	5.086 ^d , 5.108 ^e , 5.090 ^f
B_0 (GPa)	234	267 ^a , 251 ^b , 235 ^c	194 ^g , 215 ^h
E_{coh} (eV)	-15.99	-23.28 ⁱ , -11.45 ^j	-11.45 ^k , -14.72 ^l

^aRef. [27], ^bRef. [30], ^cRef. [33], ^dRef. [42],
^eRef. [43], ^fRef. [44], ^gRef. [45], ^hRef. [46],
ⁱRef. [26], ^jRef. [47], ^kRef. [48], ^lRef. [49]

The formation energies $E_F^{V_X}$ and $E_F^{I_X}$ of a vacancy (V_X) and an interstitial (I_X) of the X specie are obtained from the total energies of the system with and without the defect, according to

$$E_F^{V_X} = E^{V_{\text{ZrO}_2}} - E_{\text{ZrO}_2} + E_X, \quad (1)$$

and

$$E_F^{I_X} = E_{\text{ZrO}_2}^{I_X} - E_{\text{ZrO}_2} - E_X, \quad (2)$$

where E_{ZrO_2} is the energy of the defect-free ZrO_2 supercell, $E_{\text{ZrO}_2}^{V_X}$ and $E_{\text{ZrO}_2}^{I_X}$ are the energies of the supercell containing one vacancy and interstitial, respectively. E_X is the energy per atom of each chemical species in its reference state ($X = \text{Zr}$ or O). Here the reference state of Zr is chosen as the ground state crystalline phases, namely, the α -Zr crystal with space group $P6_3/mmc$ (No. 194). As for the O, the atomic oxygen energy is employed as a reference state [34]. In the total energy calculation of an O atom, an orthorhombic supercell with lattice constants exceeding 15 Å is employed and the spin-polarization is included. The calculated formation energy of the O vacancy in cubic ZrO_2 is in good agreement with previous theoretical and experimental results [50].

Frenkel pair consists of a non-interacting vacancy and an interstitial of the same chemical element. Thus the formation energy can be determined from the formation energies of the vacancy and of the interstitial calculated separately, given by

$$E_F^{FP_X} = E_F^{V_X} + E_F^{I_X}. \quad (3)$$

A Schottky defect is a more complex defect consisting of a Zr vacancy and two O vacancies, all of which are again supposed to be non-interacting. The formation energy is calculated by

$$E_F^{\text{Sh}} = E_{\text{ZrO}_2}^{V_{\text{Zr}}} + 2E_{\text{ZrO}_2}^{V_{\text{O}}} - 3\frac{N-1}{N}E_{\text{ZrO}_2}, \quad (4)$$

where N is the total atom number in the used supercell.

The variation in the calculated formation energies of the single point defects as a function of the size of the supercell is represented in Fig. 2. On the whole, clearly, one can see that the convergence becomes satisfied when the supercell size is chosen as large as $2 \times 2 \times 2$ (96 atoms).

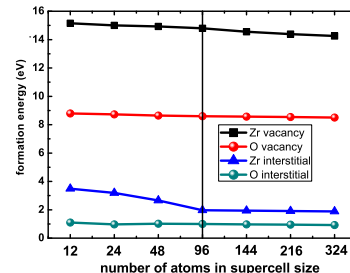


FIG. 2: Formation energies of single point defects in ZrO_2 as a function of the size of the supercell used in the calculation.

TABLE II: Calculated formation energies E_F (eV) of point defects in ZrO_2 : Zr and O vacancies (Vac), octahedral interstitials (Int), Frenkel pair (FP), and Schottky defect (Sh). The energies are calculated with atom relaxation (pos) and with atom and volume relaxation (pos+vol). $\Delta a/a$ is the variation in the lattice parameter of the 96-atom supercell.

Parameters	Int Zr	Int O	Vac Zr	Vac O	FP Zr	FP O	Sh
E_F (eV) pos	2.14	1.19	15.27	8.60	17.40	9.79	18.68
E_F (eV) pos+vol	1.97	1.17	15.26	8.60	17.22	9.77	18.66
$\Delta a/a$	0.5%	0.1%	0.1%	-0.1%	-	-	0.2%

Therefore, all the results reported in the rest of the paper are obtained with the $2 \times 2 \times 2$ supercells. Table 2 gives the formation energies of Zr and O vacancies, interstitials at OIS, Frenkel pair, and Schottky defect, all of which are obtained after performing the atom relaxation, and with or without volume relaxation. The variation in the lattice parameter $\Delta a/a$ of the supercell is also reported. This variation is only indicative of the degree of convergence of the size of the supercell: ideally, for an infinite-size supercell, this variation should be zero.

It can be seen from Table 2 that the formation energies of various point defects are positively large, consistent with the high resistance property of ZrO_2 against radiation damage. Furthermore, Table 2 shows that the O defects have much lower formation energies than Zr defects. Thus radiation damage and deviation from sto-

ichiometry will be preferably accommodated in the O sublattice: by the formation of O vacancies in hypostoichiometric ZrO_2 and by the formation of O interstitials in hyperstoichiometric ZrO_2 , for instance. The effect of volume relaxation on the formation energies is negligible, except for the Zr interstitial for which it is 0.2 eV. For this defect, the supercell size variation is the largest, but does not exceed 1%. Unfortunately, to our knowledge, the experimental values of the formation energies of point defects for cubic ZrO_2 are not available in the literature for comparison.

C. Stability of He impurity in ZrO_2

The stability of He at pre-existing trap sites is determined by calculating the incorporation energy which is defined as the energy needed to trap a He at a pre-existing trap site (vacancy or interstitial considered here) in the expression as follows:

$$E_{\text{inc}} = E_{\text{ZrO}_2}^{\text{He}} - E_{\text{ZrO}_2} - E_{\text{He}}, \quad (5)$$

where $E_{\text{ZrO}_2}^{\text{He}}$ is the energy of ZrO_2 supercell containing the He impurity, E_{ZrO_2} is the energy of the supercell with an empty trap site of He, and E_{He} is the energy of an isolated He. Therefore, a positive value means that the energy is required to incorporate He in the lattice whereas a negative result implies that incorporation is energetically favorable. A comparison of incorporation energies is the most simple way to assess the stability of the impurity and predict the most stable solution site for He provided that trap sites are available for occupation [51]. This will be the situation when the concentration of He atoms is low enough that incorporation proceeds through occupation of intrinsic defect sites.

The use of incorporation energy is limited since it is not sensitive to any equilibrium between trap sites. To take into account the equilibrium between the different trap sites one should consider solution energies. Solution energies should be used to express the population of He in the different sites when complete thermodynamical equilibrium is achieved. For a certain site X , the solution energy of He is defined as the incorporation energy plus the apparent formation energy of the trap site. It is clear that for an interstitial site incorporation and solution energies are equal. For vacancy insertion sites, the expression is given [52] as

$$E_{\text{sol}} = E_{\text{inc}} + E_{F_{\text{app}}}^{\text{V}_X}, \quad (6)$$

where $E_{F_{\text{app}}}^{\text{V}_X}$ is the apparent formation energy of the vacancy site. With stoichiometry at the ground state, the apparent formation energies of Zr and O vacancy sites can be expressed [52] as

$$E_{F_{\text{app}}}^{\text{V}_{\text{Zr}}} = E_F^{\text{Sh}} - E_F^{\text{FPo}} \quad (7)$$

TABLE III: Incorporation E_{inc} (eV) and solution energies E_{sol} (eV) of He in ZrO_2 at different sites of the fluorite lattice: the OIS, the Zr and the O substitution sites with relaxation of the atom position (pos) and volume of the supercell (vol), change in the supercell lattice parameter $\Delta a/a$, and the electron charge density Q of He at the trap sites.

Parameters	He(OIS)	He(Zr)	He(O)
E_{inc} (eV) pos	1.3491	0.4332	1.5931
E_{inc} (eV) pos+vol	1.3457	0.4199	1.5779
E_{sol} (eV) pos	1.3491	7.1327	6.4871
E_{sol} (eV) pos+vol	1.3457	7.1176	6.4650
$\Delta a/a$ (%)	0.03	0.15	0.12
Q (electrons)	2.0596	2.0298	2.1891

and

$$E_{F_{\text{app}}}^{\text{V}_O} = \frac{1}{2} E_F^{\text{FPo}}. \quad (8)$$

Here E_F^{FPo} and E_F^{Sh} are the O Frenkel pair and Schottky defect formation energies.

We investigate the He behavior at various locations including the high-symmetry positions in the lattice, and find that He always moves to the OIS during atomic relaxation in a defect-free ZrO_2 . For defective structures, we take considerations of trap sites with one Zr or O vacancy as the substitution site, respectively. The incorporation energies and solution energies are calculated by taking into account the relaxation of the atomic positions in the supercell, with and without the volume relaxation, and for the different incorporation sites. In addition, through Bader analysis [53, 54], we have also calculated the electron charge density of He when it occupies various trap sites. All the relevant results are presented in Table 3.

The calculated incorporation energies at any trap site are positive indicating that they are less stable in ZrO_2 fluorite lattice than in the free gas phase. This means that some energy has to be provided to incorporate He in ZrO_2 . The minimum incorporation energy is found for the Zr vacancy. With relatively high incorporation energies of He at OIS and O vacancy, we expect a slight preference for He to be located at Zr vacancy. However, the large solution energies at various sites (see Table 3) lead to the prediction of the insolubility of He in cubic ZrO_2 . We can conclude that the driving force for the experimentally observed He release has its origin in this insolubility. The results shows that He is more likely to be accommodated at the OIS for the thermodynamic equilibrium concentration. As for the perturbation of the crystal induced by the impurity, it is revealed that the volume relaxation with the incorporated He has no great influence on the incorporation energies and the He impurity only induces a slight expansion of the lattice parameter. Finally, Bader analysis results show that the He impurity displays only a weak charge transfer, in agreement with a complete electronic shell and neutral environment at this position. This finding also explains why

a Zr vacancy is the most favorable incorporation site for He since it is well known [55] that a He atom prefers to occupy the site with the low electron density due to its filled-shell electronic configuration.

D. Diffusion of He impurity in ZrO_2

The concentration of He remaining in the lattice is decided not only by the solution energies but also by the ease with which the He atom can diffuse out of the lattice. Here, we take considerations into the possible diffusion mechanisms for one He atom. The climbing image nudged elastic band (CINEB) method [56] is employed to find the minimum energy path (MEP) of atomic migration when both the initial and final configurations are known. The CINEB is an efficient and improved method for finding the energy saddle point between the given initial and final states of a transition to understand the energy path of He diffusion behavior. Migration energy barrier is defined as the energy difference between an initial configuration and the saddle point. The interstitial and vacancy assisted diffusion mechanisms of one He atom in ZrO_2 are systematically studied as follows.

1. interstitial diffusion mechanism

We first investigate the interstitial diffusion mechanism of He in defect-free ZrO_2 by calculating the migration energy between two adjacent OIS sites, which are the body-centered position of the lattice. The diffusion pathway and MEP are shown in Fig. 3. We perform the CINEB calculation in which the initial guess for the atomic positions of the diffusing He atom is simply a linear interpolation between the OIS sites. The saddle point obtained with this initial guess is found to be in the middle of the migration pathway as shown in Fig. 3(b), corresponding to an energy barrier of 3.74 eV. In the panel of Fig. 3(b), we can see obviously the distortion of the nearest two O atoms at the saddle point, which are pushed away from their lattice sites by about 0.37 Å in the perpendicular direction to the migration pathway of He by the strain energy.

2. Zr vacancy assisted mechanism

Next, we explore the migration pathways of He in a defective ZrO_2 and find that the energy barriers are remarkably decreased compared to the previous results. We take Zr and O vacancy into account separately to probe into the minor difference of the vacancy assisted diffusion mechanism. In the case of Zr vacancy preexisting, three possible migration pathways are assumed and CINEB calculations are carried out similarly.

The first postulated mechanism is involved in the direct diffusion of He from OIS into the nearest OIS in the

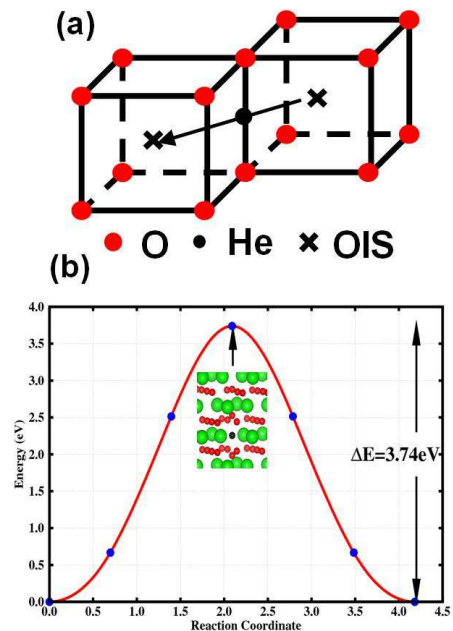


FIG. 3: (a) Diffusion pathway and (b) MEP of He migration from OIS into the nearest OIS in defectfree ZrO_2 .

presence of Zr vacancy, shown in Fig. 4(a). Examining the MEP for this mechanism in Fig. 4(b), two images on either side of the saddle point configuration exhibit a slight oscillation in energies around the transition state. The amplitude of the oscillation is only 0.02 eV, which is within the error of the calculations. The reliable estimate of the energy barrier can be obtained as about 0.23 eV, which must be overcome in the direct diffusion path of He from OIS to OIS. We find that the Zr vacancy is a trap for He atom from the MEP. Along the diffusion pathway, He atom moves into the Zr vacancy during the atomic relaxation at the third image, and an additional energy of about 1.36 eV must be provided when the He migrates back into the nearest OIS as shown in Fig. 4(b). The distortion of the nearest O atoms of He is calculated. Due to the strain energy of He, the displacement of O atom in the perpendicular direction to the pathway is about 0.43 Å at the saddle point.

The second kind of diffusion is assumed that He hops through a Zr vacancy from one OIS to the next nearest OIS. In addition, the two adjacent OIS lies in the line with Zr vacancy, represented in Fig. 5(a). It is interestingly noted that the MEP in Fig. 5(b) displays the same migration energy trend as the first one in Fig. 4(b). The energy barrier is 0.23 eV for migration from OIS to the nearest OIS, and once the He atom diffuses into the Zr vacancy, it hardly moves into the next OIS unless an extra energy of 1.36 eV is gained. The next nearest O atom has the largest distortion 0.48 Å when He is trapped in the Zr vacancy.

The third possible diffusion path is similar with the second assumption, but the two nearest OIS is not in the line with Zr vacancy, as illustrated in Fig. 6(a). We

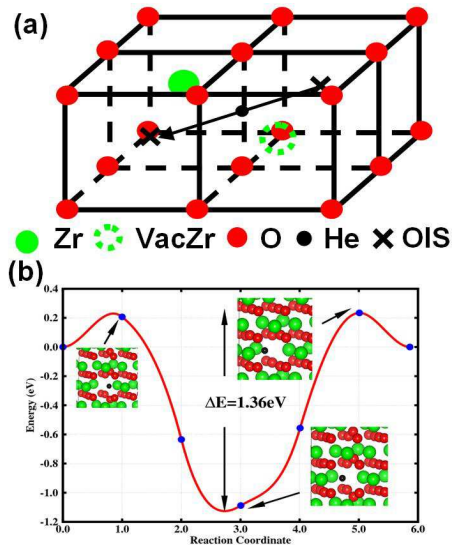


FIG. 4: (a) Diffusion pathway and (b) MEP of He migration from OIS into the nearest OIS in the presence of Zr vacancy in ZrO₂.

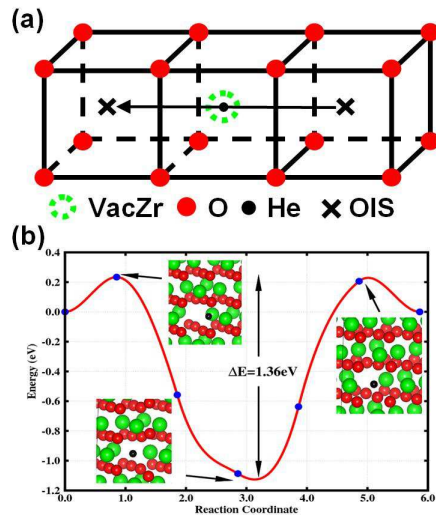


FIG. 5: (a) Diffusion pathway and (b) MEP of He migration from OIS into the next nearest OIS in the presence of Zr vacancy in ZrO₂.

consider the CINEB calculation of this migration in two steps. The MEP in Fig. 6(b) shows the step that the He atom first jumps into the Zr vacancy from the OIS, and Fig. 6(c) gives the situation that He atom migrates into the nearest OIS from Zr vacancy. From initial OIS to Zr vacancy, the saddle point is obtained with an energy barrier of 0.23 eV, and when He diffuses from Zr vacancy to final OIS, another saddle point appears with a larger migration barrier of 0.91 eV. Similarly, in this case the distortion of the nearest O atoms of He at Zr vacancy is as small as only 0.10 Å.

From above analysis, it is concluded that in ZrO₂, as Zr vacancy preexists, He diffuses easily with a lower migra-

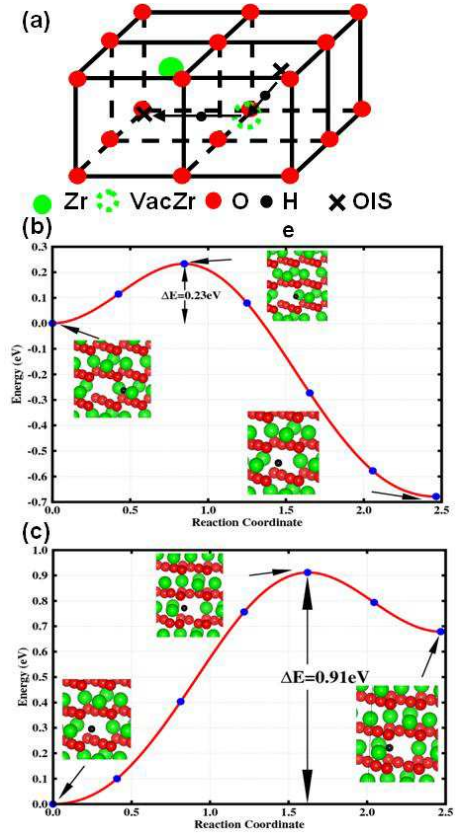


FIG. 6: (a) Diffusion pathway, (b) MEP of He migration from OIS into Zr vacancy, and (c) MEP of He migration from the Zr vacancy into the nearest OIS.

tion energy barrier than the interstitial diffusion mechanism. Different diffusion pathways proposed here demonstrate a similar migration characteristic. Obviously, it is more likely to trap the He atom into the Zr vacancy along the diffusion pathway when compared to the defect-free cases.

3. O vacancy assisted mechanism

As for O vacancy that preexists in ZrO₂, similar consideration is taken to evaluate the diffusion mechanism of He atom. At first, we discuss that He atom directly migrates from OIS into the nearest OIS, given in Fig. 7(a). Then He atom hopping from OIS to nearest OIS through O vacancy is investigated. It is considered that the He atom first moves into the O vacancy from the OIS, and next the He atom is assumed to jump into the nearest OIS from the O vacancy, shown in Fig. 8(a). The MEP of direct migration from OIS to the nearest OIS in the presence of O vacancy is different from the migration with the preexisting Zr vacancy discussed above, as shown in Fig. 7(b). There are two images in Fig. 7(b) that are predicted to be most energetically favorable. In the middle point of the pathway, the metastable state is

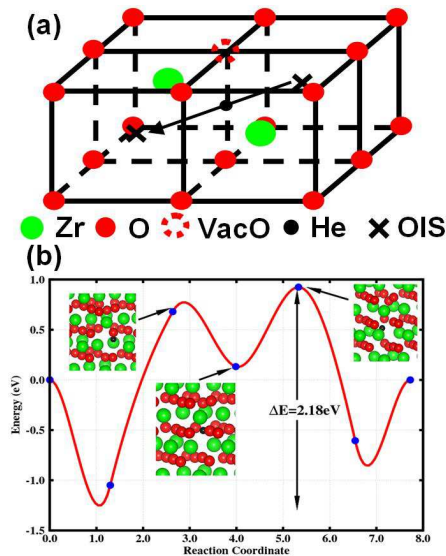


FIG. 7: (a) Diffusion pathway and (b) MEP of He migration from OIS into the nearest OIS in the presence of O vacancy in ZrO_2 .

found between the two local saddle points. At the middle image of this pathway, the He atom is trapped into the O vacancy after the relaxation during CINEB calculation. The energy barrier from the energy favorable site to the saddle point is 2.18 eV. On the other hand, the MEP of He atom hopping from OIS to nearest OIS through O vacancy is illustrated separately in Fig. 8(b) and Fig. 8(c). The saddle point is obtained in the pathway with the energy barrier 1.04 eV and 0.92 eV, corresponding the migration energy barrier from the initial OIS to O vacancy and from O vacancy to the final OIS, respectively. At various images in the CINEB calculation, the O atoms near the O vacancy move inward to the vacancy at about 0.25\AA .

From the above discussion, we find that the migration barrier of interstitial diffusion is relatively higher than the vacancy assisted diffusion. During the migration of He with Zr or O vacancy preexisted, the He atom is easily trapped into the vacancy and an extra energy of only about 1 eV is needed to hop out of the vacancy, which remarkably agrees well with the experimental result [21]. Therefore, the diffusion behavior of He atom in cubic ZrO_2 is dominated by the vacancy assisted diffusion mechanisms.

IV. CONCLUSION

In summary, we have performed total-energy calculations to investigate the formation energies of native point defects, the He incorporation and solution energies, and the diffusion properties of He in cubic ZrO_2 , using the PAW-GGA method and supercell approach. Our cal-

culated results of incorporation energies have suggested

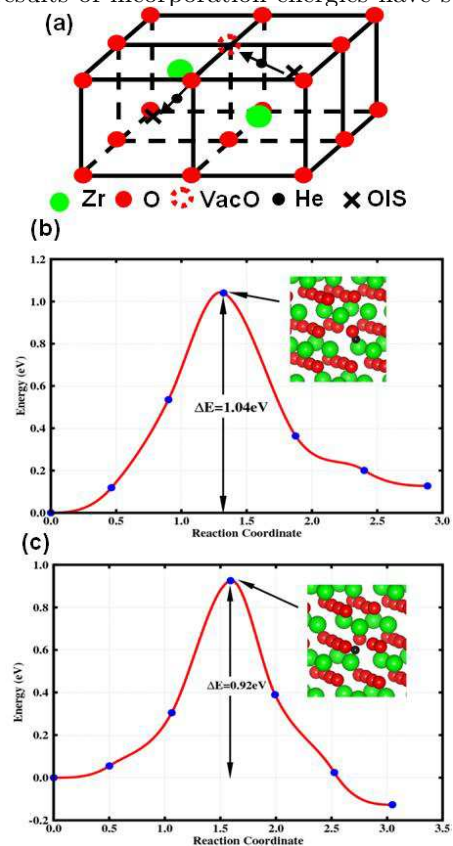


FIG. 8: (a) Diffusion pathway, (b) MEP of He migration from OIS into O vacancy, and (c) MEP of He migration from the O vacancy into the nearest OIS.

that trapping of a He atom at a Zr vacancy is more stable than at a O vacancy or at an OIS. From the solution energy results, on the other hand, it has been found that the He is more likely to be located at the OIS for the thermodynamic equilibrium concentration. To get more insights into the diffusion mechanism of He, we have calculated the migration energy of He in various pathways through the CINEB calculation, from which it has been shown once the He is trapped by the vacancy, its migration energy barrier from the vacancy to the nearest OIS is largely decreased when compared to the vacancy-free case. Thus, we conclude the diffusion of He in ZrO_2 is mainly assisted by the vacancy, which is expected to provide a guiding line in explaining the experimentally observed He diffusion phenomenon.

V. ACKNOWLEDGMENTS

This work was supported by NSFC under Grant No. 51071032 and by the National Basic Security Research Program of China.

-
- [1] G. Fadda, G. Zanzotto, and L. Colombo, *Phys. Rev. B* 82 (2010) 064105.
- [2] R. C. Garvie, R. H. Hannink, and R. T. Pascoe, *Nature* 258 (1975) 703.
- [3] M. Fèvre, A. Finel, R. Caudron, *Phys. Rev. B* 72 (2005) 104117.
- [4] L. E. Smart and E. A. Moore, *Solid State Chemistry*, Taylor and Francis, Boca Raton, 2005.
- [5] E. Curti and W. Hummel, *J. Nucl. Mater.* 274 (1999) 189.
- [6] W. L. Gong, W. Lutze, and R.C. Ewing, *J. Nucl. Mater.* 277 (2000) 239.
- [7] J. M. Leger, P. E. Tomaszewski, A. Atouf, and A. S. Pereira, *Phys. Rev. B* 47 (1993) 14075.
- [8] O. Ohtaka, T. Yamanaka, S. Kume, N. Hara, H. Asana, and F. Izumi, *Proc. Jpn. Acad., Ser. B: Phys. Biol. Sci.* 66 (1990) 193.
- [9] J. Haines, J. M. Léger, and A. Atouf, *J. Am. Ceram. Soc.* 78 (1995) 445.
- [10] J. Haines, J. M. Léger, S. Hull, J. P. Petit, A. S. Pereira, C. A. Perottoni, and J. A. H. da Jornada, *J. Am. Ceram. Soc.* 80 (1997) 1910.
- [11] H. Arashi, T. Yagi, S. Akimoto, and Y. Kudoh, *Phys. Rev. B* 41 (1990) 4309.
- [12] O. Ohtaka, T. Yamanaka, and T. Yagi, *Phys. Rev. B* 49 (1994) 9295.
- [13] M. C. Wittels and F. A. Sherrill, *Phys. Rev. Lett.* 3 (1959) 176.
- [14] K. E. Sickafus, H. Matzke, Th. Hartmann, K. Yasuda, J. A. Valdez, P. Chodak III, M. Nastasi, R. A. Verrall, *J. Nucl. Mater.* 274 (1999) 66.
- [15] A. Meldrum, L. A. Boatner, and R. C. Ewing, *Phys. Rev. Lett.* 88 (2002) 025503.
- [16] G. Kuri, M. Döbeli, D. Gavillet, *Nucl. Instr. and Meth.* 245 (2006) 445.
- [17] G. Kuri, D. Gavillet, M. Döbeli, D. Novikov, *Nucl. Instr. and Meth.* 266 (2008) 1216.
- [18] G. Kuri, C. Degueldre, J. Bertsch, M. Döbeli, *Nucl. Instr. and Meth.* 268 (2010) 2177.
- [19] G. Velisa, A. Debelle, L. Vincent, L. Thomé, A. Declémy, D. Pantelica, *J. Nucl. Mater.* 402 (2010) 87.
- [20] S. Saudé, R. I. Grynszpan, W. Anwand, G. Brauer, J. J. Grob, Y. Le Gall, *Nucl. Instr. and Meth.* 216 (2004) 156.
- [21] P. M. G. Damen, H. Matzke, C. Ronchi, J. P. Hiernaut, T. Wiss, R. Fromknecht, A. van Veen, F. Labohm, *Nucl. Instr. and Meth.* 191 (2002) 571.
- [22] J. M. Costantini, J. J. Grob, J. Haussy, P. Trocellier, Ph. Trouslard, *J. Nucl. Mater.* 321 (2003) 281.
- [23] H. J. F. Jansen, *Phys. Rev. B* 43 (1991) 7267.
- [24] R. Orlando, C. Pisani, C. Roetti, and E. Stefanovich, *Phys. Rev. B* 45 (1992) 592.
- [25] R. H. French, S. J. Glass, F. S. Ohuchi, Y. N. Xu, and W. Y. Ching, *Phys. Rev. B* 49 (1994) 5133.
- [26] G. Jomard, T. Petit, A. Pasturel, L. Magaud, G. Kresse, and J. Hafner, *Phys. Rev. B* 59 (1999) 4044.
- [27] J. E. Lowther, J. K. Dewhurst, J. M. Léger, and J. Haines, *Phys. Rev. B* 60 (1999) 14485.
- [28] J. K. Dewhurst and J. E. Lowther, *Phys. Rev. B* 57 (1998) 741.
- [29] L. K. Dash, N. Vast, P. Baranek, M. C. Cheynet, and L. Reining, *Phys. Rev. B* 70 (2004) 245116.
- [30] J. E. Jaffe, R. A. Bachorz, and M. Gutowski, *Phys. Rev. B* 72 (2005) 144107.
- [31] M. Sternik and K. Parlinski, *J. Chem. Phys.* 122 (2005) 064707.
- [32] Akihide Kuwabara, Tetsuya Tohei, Tomoyuki Yamamoto, and Isao Tanaka, *Phys. Rev. B* 71 (2005) 064301.
- [33] G. Fadda, L. Colombo, and G. Zanzotto, *Phys. Rev. B* 79 (2009) 214102.
- [34] A. S. Foster, V. B. Sulimov, F. Lopez Gejo, A. L. Shluger, and R. M. Nieminen, *Phys. Rev. B* 64 (2001) 224108.
- [35] J. X. Zheng, G. Ceder, T. Maxisch, W. K. Chim, and W. K. Choi, *Phys. Rev. B* 75 (2007) 104112.
- [36] C. Àrhammar, C. Moysés Araújo, and Rajeev Ahuja, *Phys. Rev. B* 80 (2009) 115208.
- [37] P.E.Blöchl, *Phys. Rev. B* 50 (1994) 17953.
- [38] G. Kresse, J. Furthmüller, *Phys. Rev. B* 54 (1996) 11169.
- [39] J.P.Perdew, K.Burke, M.Ernzerhof, *Phys. Rev. Lett.* 77 (1996) 3865.
- [40] H.J.Monkhorst, J.D.Pack, *Phys. Rev. B* 13 (1972) 5188.
- [41] F. Birch, *Phys. Rev.* 71 (1947) 809.
- [42] C. J. Howard, R. J. Hill, and B. E. Reichert, *Acta Crystallogr., Sect. B: Struct. Sci.* B44 (1988) 116.
- [43] N. Igawa, Y. Ishii, T. Nagasaki, Y. Morii, S. Funahashi, and H. Ohno, *J. Am. Ceram. Soc.* 76 (1993) 2673.
- [44] E. V. Stefanovich, A. L. Shluger, and C. R. A. Catlow, *Phys. Rev. B* 49 (1994) 11560.
- [45] H. M. Kandil, D. Greiner, and J. F. Smith, *J. Am. Ceram. Soc.* 67 (1984) 341.
- [46] R. P. Ingel and D. Lewis, *J. Am. Ceram. Soc.* 71 (1988) 265.
- [47] N. I. Medvedeva, V. P. Zhukov, M. Y. Khodos, and V. A. Gubanov, *Phys. Stat. Sol. (b)* 160 (1990) 517.
- [48] G. V. Samsonov (Ed.), *Fiziko-khimicheskie svoistva oksidov*, Izd. Metallurgiya, Moskva 1978.
- [49] D. G. Pettifor, *J. Phys. F* 7, (1977) 613.
- [50] T. Bredow, *Phys. Rev. B* 75 (2007) 144102.
- [51] S. E. Donnelly, J. H. Evans (Eds), *Fundamental Aspects of Inert Gases in Solids*, Plenum, New York, 1991.
- [52] J. P. Crocombette, *J. Nucl. Mater.* 305 (2002) 29.
- [53] W.F.W.Bader, *Atoms in Molecules: A Quantum Theory*, Oxford University Press, New York, 1990.
- [54] W.Tang, E.Sanville, G.Henkelman, *J.Phys.: Condens. Matter* 21 (2009) 084204.
- [55] M. J. Puska, R. M. Nieminen, *Phys. Rev. B* 43 (1991) 12221.
- [56] G. Henkelman, B. P. Uberuaga, and H. Jonsson, *J. Chem. Phys.* 113 (2000) 9901.